

Large hadron collider physics program: Compact muon solenoid experiment

J B SINGH

Physics Department, Panjab University, Chandigarh 160 014, India

Abstract. The LHC physics program at CERN addresses some of the fundamental issues in particle physics and CMS experiment would concentrate on them. The CMS detector is designed for the search of Standard Model Higgs boson in the whole possible mass range. Also it will be sensitive to Higgs bosons in the minimal supersymmetric model and well adapted to searches for SUSY particles, new massive vector bosons, CP-violation in B -system, search for substructure of quarks and leptons, etc. In the LHC heavy ion collisions the energy density would be well above the threshold for the possible formation of quark–gluon plasma.

Keywords. Higgs boson; SUSY; QGP; LHC; CMS.

PACS Nos 14.80; 13.85; 12.38; 12.60

1. Introduction

The large hadron collider (LHC) at CERN would be the most powerful accelerator ever built smashing the protons on protons at $\sqrt{s} = 14$ TeV at the luminosity 2.5×10^{34} $\text{cm}^{-2}\text{sec}^{-1}$ [1]. The LHC physics programme represents the only facility in the near future to probe and solve present fundamental puzzles in particle physics namely: search for Standard Model Higgs boson up to the whole possible mass range 1000 GeV, search for Higgs bosons in the minimal supersymmetric model (MSSM), SUSY particles, new massive vector bosons, the origin of spontaneous symmetry breaking (SSB) mechanism in electroweak sector of the Standard Model, possibility of more fundamental constituents in nature, search for definite signature of quark gluon plasma (QGP) in the heavy ion collisions, etc.

The cross-sections for most of these relevant processes are minute compared to the total inelastic cross-sections and extraction of small signal over a huge background is very difficult. So to explore these processes accelerator and detectors are to be very complex and the requirements for the detector performance are extreme. From this point of view, the detector fabrication is very crucial. The compact muon solenoid (CMS) has been designed to cover most effectively the above mentioned physics aspects [2], together with the other multipurpose detector ATLAS [3].

The main features of LHC accelerator machine along with experiments to be performed with this are presented in §2. A detailed description of different detector components of CMS detector is being discussed in §3. In §4, various physics potentials of LHC/CMS

are presented and particular emphasis has been given to Higgs boson search, CP-violation in B -system and search for signature of quark gluon plasma in CMS using heavy ion collisions.

2. The LHC machine

The large hadron collider (LHC) being constructed at CERN would be operational in 2005. The LHC will collide counter-rotating beams of protons with total center of mass energy 14 TeV. Since interesting physics have very small cross-sections (e.g. Higgs and Z' \approx 1 pb), there is a need for high luminosity. To achieve very high luminosity at LHC, at a time there would be 3000 bunches in the machine, each bunch having 10^{11} protons. The separation between two bunches would be 25 nsec (\approx 7.5 m) leading to \approx 18 proton-proton interactions for each bunch crossing. These design LHC parameters would provide maximum luminosity of $2.5 \times 10^{34} \text{ cm}^{-2}\text{sec}^{-1}$ which will give 2.5×10^9 interactions per second. The LHC energy and luminosity would be an order of magnitude higher than present collider machines. Thus much higher energy and luminosity of LHC would make possible the search of new massive particles produced with small cross-sections and probe the structure of matter at extremely small distance scales.

2.1 Experiments at LHC

At LHC machine two multipurpose detectors CMS and ATLAS would carry out studies of proton-proton interactions. Indian groups from BARC, EHEP-TIFR, HECR-TIFR, Panjab and Delhi Universities are participating in LHC physics program of CMS. These groups are involved at all the stages of CMS experiment, starting from design, R&D, production phase, testing and final installation at CERN. Another aspect of the LHC machine is its use as collider of relativistic heavy ions for the search of quark gluon plasma. A dedicated experiment ALICE would study this physics, where Indian groups are also involved [4]. For the dedicated B -physics studies LHCb detector has been designed [5]. In the present article the LHC physics program is discussed in reference to CMS experiment.

3. The CMS experiment

The compact muon solenoid (CMS) is a general purpose proton-proton interaction detector designed to run at the highest luminosity at the LHC. The main design goals of CMS are a highly performant muon system, the best possible electromagnetic calorimeter, high quality central tracking system and hadron calorimeter. These detector components have been optimized to detect cleanly the diverse signatures from new physics by identifying and precisely measuring muons, electrons, photons and hadron jets over a large energy range. The CMS is a 12,500 tons, 22 m long and 15 m diameter detector having 4 Tesla superconducting solenoid magnet. A central tracking system, a high resolution PbWO_4 crystal electromagnetic calorimeter and a copper-plastic scintillator hadron calorimeter reside inside the magnet coil; a robust muon detection system with 4 layers of muon stations will surround the magnet. Figure 1 shows longitudinal view of the proposed CMS detector. The key elements of CMS detector are described briefly and its anticipated performance for the main benchmark physics processes.

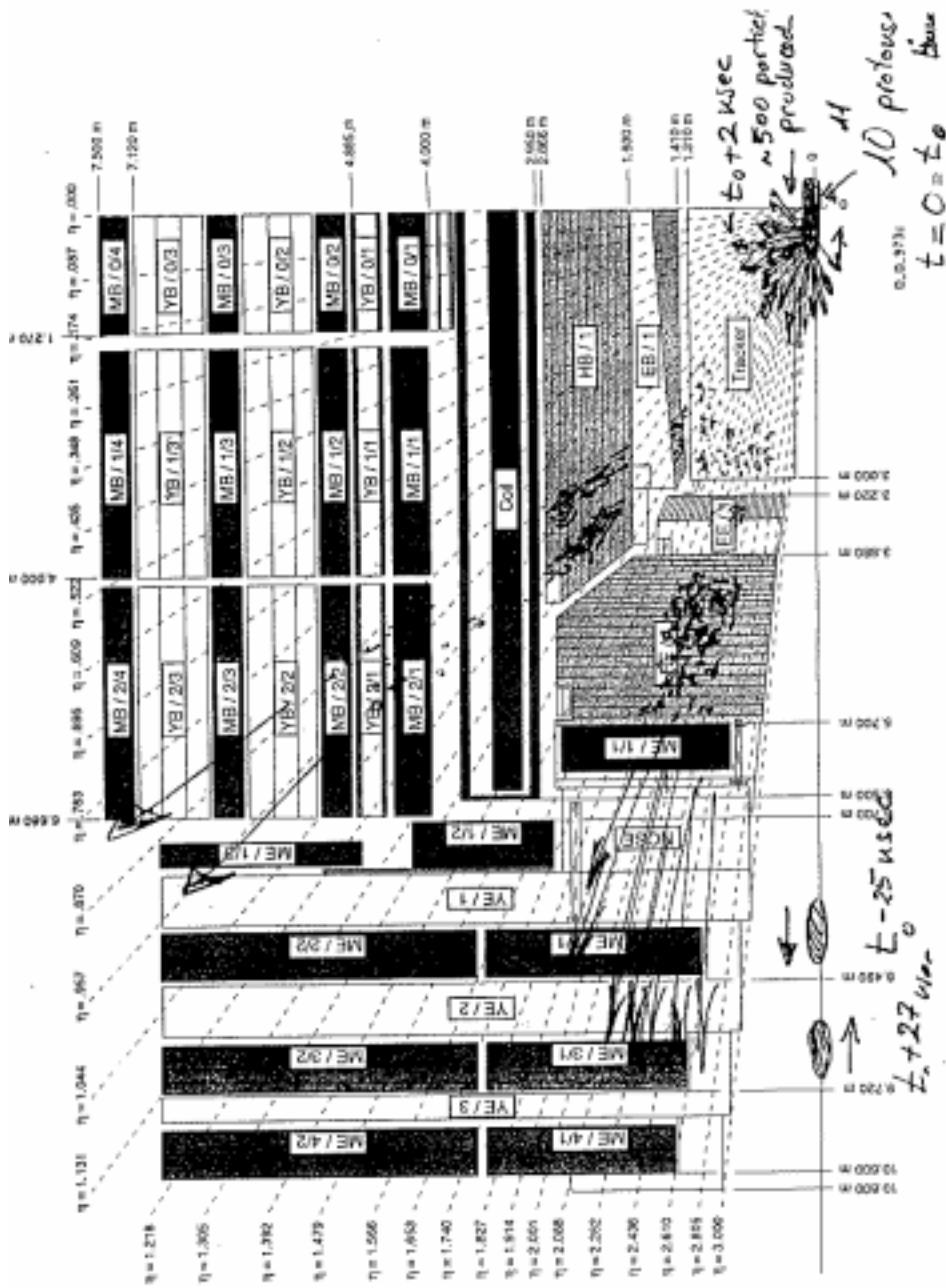


Figure 1. Longitudinal view of the CMS detector.

3.1 Magnet

For CMS detector a solenoid configuration has been chosen for the magnet because the bending of charged particle trajectories starts at the beam axis and this minimises the detector size for a given bending power. So a long superconducting solenoid of length 13 m and inner diameter 5.9 m, with a uniform magnetic field of 4 T, has been chosen. The inner coil diameter is large enough to accommodate the tracker and calorimeter.

3.2 Central tracking system

The goal of the CMS tracking system is to reconstruct high P_T muons, isolated electrons and charged hadrons in the central rapidity region and to determine the charge-sign of particles with energies up to 2 TeV. Particular emphasis has been given to reconstruct isolated high- P_T muons and electrons with a momentum resolution better than $\Delta P_T/P_T \approx 0.1 P_T$ (TeV/c) with high efficiency over a wide range of rapidities. This value was defined using benchmark processes for the detection of an intermediate mass Higgs boson $H \rightarrow ZZ^*/ZZ \rightarrow 4l^\pm$. The high momentum resolution minimizes all possible background contributions under the mass peak and high momentum precision is a direct consequence of the high magnetic field. The tracking volume is given by a cylinder of length 7 m and diameter 2.6 m which consists of three components namely: (1) silicon pixel detectors, (2) silicon strip detectors and (3) microstrip gas chambers (MSGC). In the barrel region a track with reasonable high momentum ($P_T > 5$ GeV/c) will first cross 2-layers of Si-pixels which has $r - \phi$ pitch of $150 \mu\text{m} \times 150 \mu\text{m}$, then 3-layers of Si-strips with a pitch of $60/83/125 \mu\text{m}$ and finally 7-layers of MSGCs with a pitch of $200 \mu\text{m}$. The expected resolution per point is typically $15 \mu\text{m}$ for silicon detector and better than $50 \mu\text{m}$ for the MSGCs. In the forward and backward region tracking detectors are configured in the form of discs.

With these parameters, performance of the tracks through CMS tracking detector is simulated and tracking efficiency is typically 98% for an isolated track, whereas tracks inside the jets can be found with an efficiency of $> 95\%$. The tagging efficiency for b -jets varies between 20 and 50%, while mistagging probability is between 0.04 and 1.9%. Along with muon system, the muon momentum resolution is better than 5% at 0.3 TeV in the central rapidity region $|\eta| < 2$ and 10% for $P_T = 2$ TeV. The low momentum ($p_T < 100$ GeV) muons are measured before the absorber with a precision of about 1.5% up to $\eta < 2$.

3.3 Electromagnetic calorimeter (ECAL)

The relevant benchmark process to define the necessary properties of the ECAL is $\text{Higgs} \rightarrow \gamma\gamma$ for the mass range 80–160 GeV. So precision energy and direction measurement of photon is required. Thus ECAL has been chosen with a granularity of $\Delta\phi \times \Delta\eta = 0.017 \times 0.017$. This will be achieved by high precision ECAL using lead tungstate (PbWO_4) crystals. The crystal would have projected tower geometry each 230 mm in length ($25.8 X_0, 1.1\lambda$) and $\approx 22 \times 22$ mm in cross-section. The time constant of scintillation light coming from lead tungstate crystals is only 10 nsec. In CMS light will be detected by Si-avalanche photodiodes which can provide gain of 50 even in high magnetic field environment.

In order to facilitate γ/π^0 separation in the forward–backward region ($1.66 \leq |\eta| \leq 2.61$) a pre-shower silicon strip detector is included in the baseline CMS design. These detectors would be placed just in front of the two crystal endcap modules. This gives accurate information about the starting position of an EM shower, whilst the location of shower center is determined from energy distribution of the calorimeter cells. Indian groups are involved in this activity also.

3.4 Hadron calorimeter (HCAL)

The relevant benchmark processes which define the HCAL performance requirements are decays of massive Higgs bosons $H \rightarrow WW \rightarrow l\nu l\nu$, $H \rightarrow ZZ \rightarrow lljj$ and $Z' \rightarrow jj$. Since these processes suffer from heavy background, in addition to leptons one or two forward going jets will be used as a tagging of Higgs. So the factors that determine the required performance of HCAL are jet energy and E_T^{miss} resolution.

The central rapidity range ($|\eta| < 3.0$) is covered by the hadron calorimeter barrel (HB) and endcap (HE) as shown in figure 1, which is sampling calorimeter. It consists of plastic scintillator as active material inserted between copper absorber plates. The absorber plates are 5 cm thick and plastic scintillator tiles 4 mm thick. The scintillator tiles are read out individually by green wavelength shifting fibers coupled to clear plastic fibers which transports the light to the transducers outside the calorimeter. Since calorimeter would be in a high magnetic field, so hybrid photodiodes (HPD) would be used. The HCAL tiles are arranged in projected towers geometry of granularity $\Delta\phi \times \Delta\eta = 0.087 \times 0.087$.

Because of narrow space in the magnetic coil, HCAL resides between 1.9 m and 2.9 m radially equivalent to 89 cm in sampling depth ($\approx 5.8\lambda$), which is somewhat thin. Figure 2 presents the total thickness of HCAL in terms of number of nuclear interaction lengths (λ) as a function of η . As seen from the figure, for hadrons emitted at 90° ($\eta = 0$) the nuclear interaction length is ≈ 7 including ECAL. This is not sufficient for complete hadronic shower containment. Hence it is necessary to extend the barrel part of HCAL beyond magnet and make additional sampling of the shower. This is essential to improve the missing E_T resolution [6].

With this aim, outer hadron calorimeter (HO) has been included in CMS baseline design with two layers of scintillator. Figure 2 shows the reconstructed energy distribution for pions of $E_T = 200$ GeV without and with HO layers. A clear suppression of the low energy tail is seen with the addition of HO layers. These measurements were supported by the test beam data analysis [6]. This extended HCAL HO is very crucial for the search of SUSY particles and high mass Higgs boson. One layer of the HO would be stationed just after magnet coil at 3.82 m radially (Layer 0) and another (Layer 1) at 4.07 m before the muon stations (MB0) (figure 1) [6,7].

Indian groups have taken up full responsibility of this HO detector project.

A large rapidity coverage up to ($|\eta| = 5$) is required to measure the E_T^{miss} which is needed to detect forward jets. So CMS employs a separate forward calorimeter (HF) located 6 m downstream of the HE endcaps. The HF calorimeter covers the region $3.0 < |\eta| < 5.0$. It uses the quartz fibers as the active medium embedded in a copper absorber matrix.

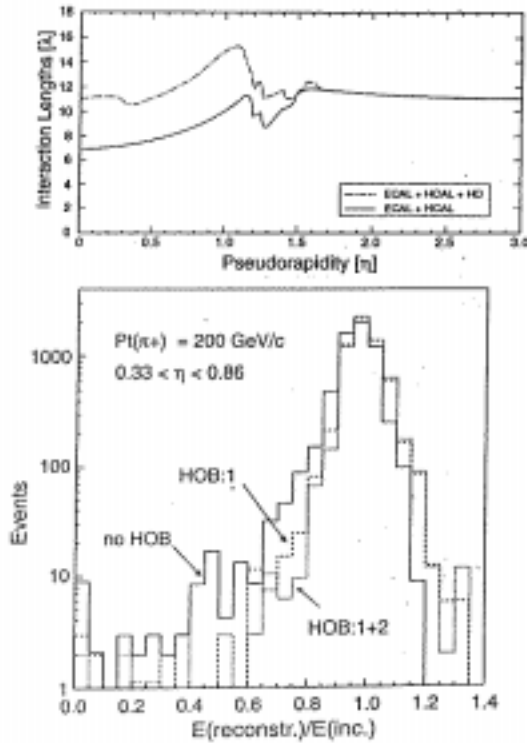


Figure 2. Thickness of calorimeter system and single π response with and without HO detector.

3.5 Muon chambers

Since its inception, CMS has put highest emphasis on its muon system which should provide high quality muon reconstruction. To effectively detect muons from Higgs boson, W , Z and $t\bar{t}$ decays, the acceptance of the system has to extend over a wide range of rapidity. To guarantee sharp trigger thresholds and a robust momentum measurement, the system has to have a high momentum resolution in its standalone mode. So for the best muon detection and momentum measurement it was decided to use four separate muon stations inserted in the solenoid return yoke MB1-MB4 in barrel shown in figure 1. Each muon station consists of three groups of four planes of drift tubes. Two groups measure the $(r - \phi)$ coordinate and one group measure Z . Each station measures a muon vector in space, with $100 \mu\text{m}$ precision in position and better than 1 mrad in Z -direction. Because of the high rates and high magnetic field in the endcap region cathode strip chambers were chosen for the endcap muon system (ME), since these devices are capable of working even in high magnetic field.

The muon chambers are arranged in such a way that all muon tracks traverse four stations at all rapidities. The space resolution of muon system are $200 \mu\text{m}$ per plane for barrel and $100 \mu\text{m}$ for endcap. The measurement of muon momentum are made three times inside

the central tracker, after the coil and in the iron return yoke. So the muon momentum measurements remains accurate in the full rapidity range because of high bending power of the solenoid. The momentum resolution is better than 5% for 1 TeV and $\approx 10\%$ for $p_T = 2$ TeV in the central rapidity region. The typical mass resolution using the combined muon-tracker system are 16 MeV for $\phi \rightarrow \mu\mu$; 1 GeV for $H \rightarrow ZZ^*$; 1.8 GeV for $Z^0 \rightarrow \mu\mu$ from a 300 GeV Higgs decay, and 150 GeV for a 3 TeV, $Z' \rightarrow \mu^+\mu^-$.

4. Physics at LHC

The fundamental physics program of LHC and CMS detector is to uncover and explore the physics behind the electroweak symmetry breaking. Amongst others some of them involve the following specific challenges:

- Standard Model Higgs boson search at masses above the maximum reach of LEP and Tevatron, order of 100–1000 GeV.
- Minimum Supersymmetric Standard Model (MSSM) Higgs bosons searches up to masses 2.5 TeV. In the framework of the MSSM, five Higgs bosons (h^0, H^0, A^0, H^\pm) are expected.
- Search for new heavy gauge bosons (W', Z') up to masses 4.5 TeV
- Search for SUSY partners of quarks and gluons-squark and gluino up to masses 2.5 TeV.
- Search for composite structures of quarks and leptons
- Study of CP-violation and time-dependent mixing of b -mesons
- Detailed studies of production and decays of top quark
- Tests of EW gauge couplings-triple gauge boson vertices
- Search for quark gluon plasma (QGP) in heavy ion collisions

In the subsequent sections the discovery potential of SM Higgs boson in CMS would be discussed in detail and a brief discussion on CP-violation in B -meson system and search for QGP would be given.

4.1 Search for Standard Model Higgs boson

The LEP-II run at 195–200 GeV can extend the Higgs mass search reach up to $M_H = 95$ –105 GeV [8,9]. Also Tevatron collider would not be able to extend the Higgs mass reach beyond LEP-II. Thus Higgs mass range of interest to LHC would be $M_H > 95$ GeV.

4.2 Production of the Standard Model Higgs boson

According to present theoretical understanding, the Standard Model Higgs boson at proton–proton colliders can be produced through four possible mechanisms: (i) gluon–gluon fusion, $gg \rightarrow H$; (ii) WW or ZZ fusion, $qq \rightarrow Hqq$; (iii) $t\bar{t}$ fusion, $gg \rightarrow Ht\bar{t}$, $q\bar{q} \rightarrow Ht\bar{t}$; (iv) W or Z bremsstrahlung, $q\bar{q} \rightarrow HW/HZ$ [10,11]. The Feynman diagrams of these processes alongwith the production cross-sections are displayed in figure 3

[11,12]. As seen from the figure, at LHC the dominant production mechanism up to Higgs mass ≈ 700 GeV is the gluon-gluon fusion via top quark loop and at $M_H = 100$ GeV cross-section is ≈ 60 pb. The WW or ZZ fusion mechanism becomes important for the production of Higgs boson beyond ≈ 300 GeV and rate becomes comparable with gluon-gluon fusion at ≈ 700 GeV. The W or Z bremsstrahlung mechanism does not play much role for Higgs boson beyond ≈ 90 GeV.

The associated production $gg \rightarrow t\bar{t}H$ or $q\bar{q} \rightarrow WH$ or ZH is significant for low mass Higgs boson (~ 100 GeV). The detailed signal and background simulations for various Higgs processes can be seen in [2]. The number of expected events for each mechanism are also shown in figure 3 for an integrated luminosity of 10^5 pb^{-1} which corresponds to about one year running of LHC.

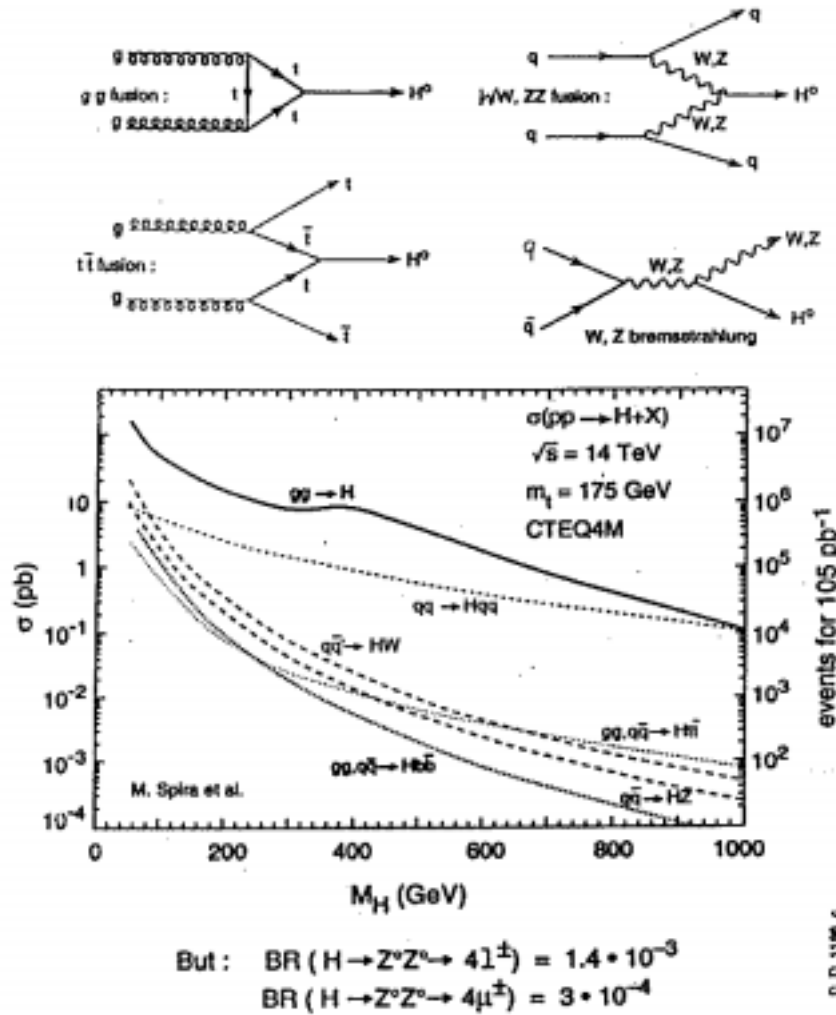


Figure 3. Higgs boson production mechanisms and production cross-sections at LHC.

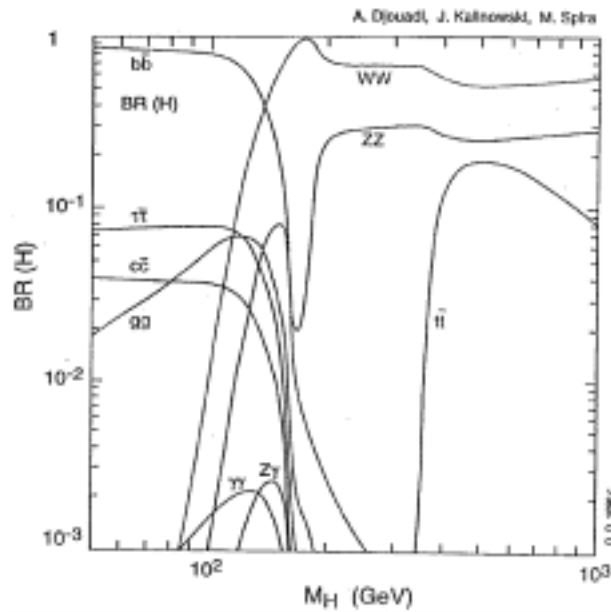


Figure 4. Standard Model Higgs boson decay branching ratios.

4.3 Detection of Standard Model Higgs boson

According to various SM Higgs boson decays, the branching ratios for the important decay channels are shown in figure 4. The Higgs mass search reach can be divided into several parts depending upon its expected observability into different search modes which is discussed in subsequent sections.

4.3.1 Higgs $\rightarrow b\bar{b}$

As seen from the decay branching ratio results, for Higgs mass up to 160 GeV, this decay mode is most dominant having largest branching ratio, 10–20 times compared to other channels (figure 4). But unfortunately this decay mode has huge QCD background ≈ 1000 times larger than the signal. So this channel is not usable for the search of Higgs boson at LHC and can be important for the searches below 100 GeV. Still, silicon pixel devices of CMS will certainly open the way for this search and signal evaluation are under way.

4.3.2 Higgs $\rightarrow \gamma\gamma$

The CMS detector having very good EM calorimetry, capable of measuring the γ energy and direction to 1% accuracy, is expected to extend the Higgs search up to mass $M_H = 150$ GeV with this decay mode. The detector simulated 100 GeV Higgs boson decaying via this channel has been seen without any ambiguity in the CMS detector. A background subtracted simulated two-photon effective mass plot for an integrated luminosity of 10^5 pb^{-1} with signals at Higgs mass $M_H = 90, 110, 130$ and 150 GeV is shown in figure 5.

As seen from figure the background can be reduced significantly with proper isolation and E_T cuts.

The decay channel $H \rightarrow \gamma\gamma$ has the cleanest signal but suffers from the small branching ratio 1000 times smaller than most of the other channels (figure 4). The largest Higgs production cross-section via gluon-gluon fusion is of the order of 10 pb (figure 3). The expected size of the signal for $H \rightarrow \gamma\gamma$ is 10 fb which corresponds to 10^3 events. The estimated background is 10^4 events which can be subtracted out with suitable methods.

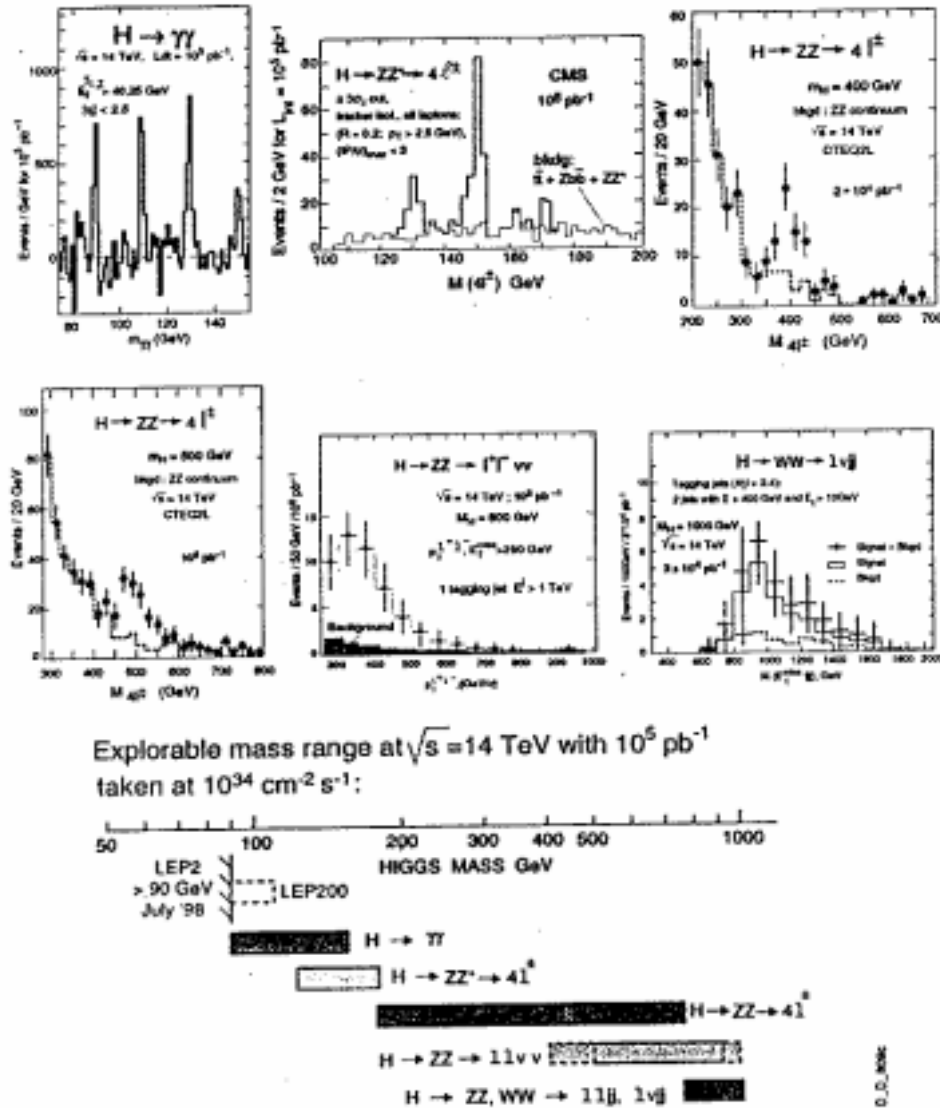


Figure 5. Higgs searches in different detection modes and explorable mass range at LHC.

Thus the significance of the signal relative to its size with statistical uncertainty in the background is ($N_S/\sqrt{N_B} \approx 10$). Figure 6 shows the contours giving this signal significance as a function of Higgs mass. After a single year running of LHC and CMS collecting integrated luminosity of 10^5 pb^{-1} , Higgs would be discovered through this channel across the full mass reach 85–150 GeV.

4.3.3 Higgs $\rightarrow ZZ^*/ZZ \rightarrow 4l^\pm$

The most promising Higgs decay channel for its search in the higher mass range is $H \rightarrow ZZ/ZZ^* \rightarrow l^+l^-l^+l^-$. The reconstruction of the l^+l^- invariant mass makes it practically background free and has very significant branching ratio (figure 4). Thus it provides the most important Higgs signal for $M_H = 130\text{--}750 \text{ GeV}$. The robust CMS muon detector and ECAL would detect 4-muons/electrons cleanly. Figure 5 shows results from a simulation with reconstructed Higgs signals through 4-charged leptons at masses $M_H = 130, 150$ and 170 GeV . Using appropriate transverse energy cuts on electrons and P_T cuts on muons, background can be reduced significantly and clean Higgs signal is seen (figure 5).

The high mass Higgs boson at $M_H = 400$ and 500 GeV were also simulated and results of background subtracted 4-charged leptons effective mass is shown in figure 5 and signal is much cleaner. Since in this high mass region sources of background is from ZZ only which is easy to be removed. Figure 6 shows the expected signal significance ($N_S/\sqrt{N_B}$).

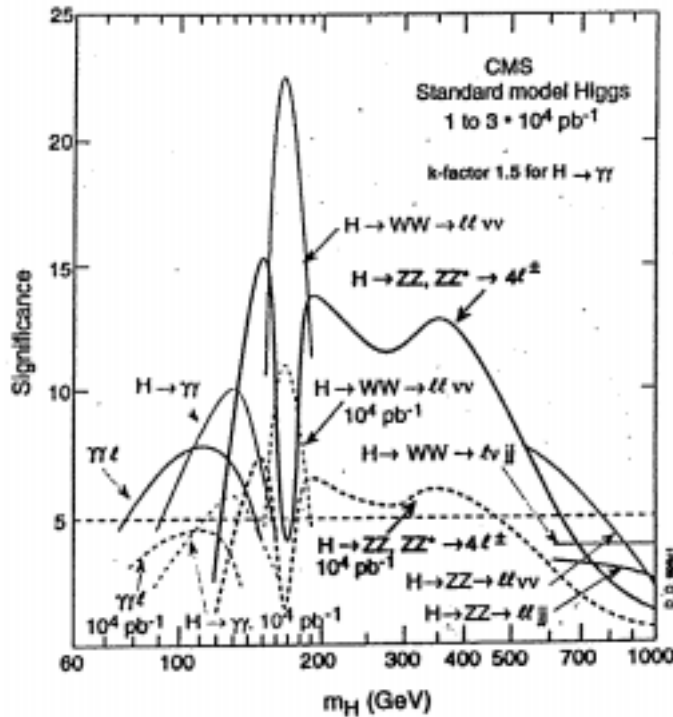


Figure 6. Expected observability of SM Higgs boson and mass range reach in CMS.

As seen from the figure the discovery region extends up to $M_H = 800$ GeV. Also this search mode has maximum Higgs mass search range.

4.3.4 *Higgs* $\rightarrow WW \rightarrow 2l^\pm 2\nu$

Another important channel is $H \rightarrow WW \rightarrow 2l^\pm 2\nu$ for $M_H = 130-200$ GeV mass window. This channel has highest branching ratio, six times larger than $H \rightarrow ZZ \rightarrow 4l^\pm$. Also it has a distinct signature, two high p_T leptons and high E_T^{miss} [13]. The CMS detector having very good ECAL and muon system would be able to give clean reconstructed electrons/muons coming from this decay modes. The missing transverse energy due to 2ν would be provided by very good CMS calorimetry giving rise to practically background free signal, in spite of large background from $t\bar{t}$ decay.

4.3.5 *Higgs* $\rightarrow ZZ \rightarrow 2l^\pm jj$ and *Higgs* $\rightarrow WW \rightarrow l\nu jj$

However for large Higgs mass $M_H = 500-1000$ GeV, the 4-charged leptons signal becomes too small. In this case the decay channels $H \rightarrow WW \rightarrow l^\pm \nu jj$, $H \rightarrow ZZ \rightarrow l^+ l^- \nu \nu$ and $H \rightarrow ZZ \rightarrow l^+ l^- jj$ are expected to provide more favourable signals. In these channels biggest background comes from single W (or Z) production along with QCD jets. This background can be removed by selecting accompanied two forward jets, since a large part of the signal cross-section in this case comes from WW fusion, which is accompanied with two forward jets. So one can use double forward jet tagging to control the background [14]. The CMS simulation studies show that using this strategy one can extend the Higgs search up to 1 TeV [2,14,15].

4.4 *Explorable mass range of Higgs boson*

The background subtracted expected signals for above discussed search channels and at relevant Higgs masses with 10^5pb^{-1} simulated data is shown in figure 5. Also figure shows the explorable Higgs mass reach through these channels at LHC. In figure 6 the expected observability of SM Higgs in CMS experiment with 10^5pb^{-1} taken at $10^{34} \text{cm}^{-2} \text{sec}^{-1}$ is presented for possible Higgs detection modes.

To summarize the explorable Higgs mass ranges through various decay channels can be arranged:

| | |
|--|---------------------------------|
| $H \rightarrow \gamma\gamma$ | for $80 \leq M_H \leq 140$ GeV |
| $H \rightarrow ZZ^* \rightarrow 4l^\pm$ | for $130 \leq M_H \leq 200$ GeV |
| $H \rightarrow ZZ \rightarrow 4l^\pm$ | for $200 \leq M_H \leq 750$ GeV |
| $H \rightarrow ZZ \rightarrow 2l^\pm 2\nu$ | for $0.5 \leq M_H \leq 1$ TeV |
| $H \rightarrow WW \rightarrow l^\pm \nu l^\pm \nu$ | for $140 \leq M_H \leq 200$ GeV |
| $H \rightarrow WW \rightarrow l^\pm \nu jetjet$ | for $M_H \approx 1$ TeV |
| $H \rightarrow ZZ \rightarrow l^\pm l^\pm jetjet$ | for $M_H \approx 1$ TeV |

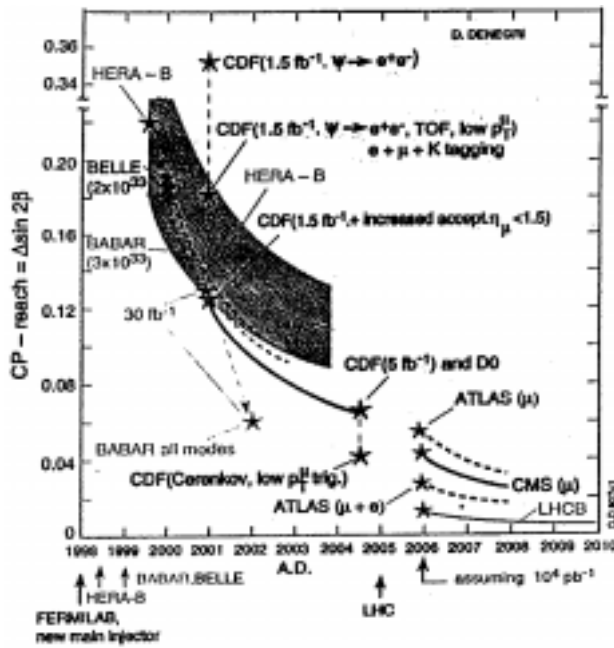


Figure 7. CP-violation reach of CMS in $B_d^0 \rightarrow \phi K_s^0$.

4.5 CP-violation in the B-meson system

The LHC would also be working as a B -factory, producing 10^{12} – $10^{13} b\bar{b}$ per year, which would open the way for precise measurements of parameters characterizing the CP-violation effects in the B -system. The CMS detector having very good tracking, calorimetry and muon system, would be able to detect most promising decay channels which have small branching ratios like, $B_d^0 \rightarrow J/\psi K_s^0$ and $B_d^0 \rightarrow \pi^+ \pi^-$; with $J/\psi \rightarrow \mu^+ \mu^-$ and $K_s^0 \rightarrow \pi^+ \pi^-$. These channels would measure two β and α angles of the unitarity triangle. The first reaction has a relatively high branching ratio and clear signature. It is easier to trigger on multi-muon with low p_T or a single muon. With an integrated luminosity of 10^4 pb^{-1} in CMS, an accuracy in the measurements of $\sin 2\alpha = 0.057$ and $\sin 2\beta = 0.05$ can be achieved. In figure 7 the expected experimental uncertainty ($\Delta \sin 2\beta$) on measurement of CP-violation parameter $\sin 2\beta$ in various experiments are compared with CMS. Both LHC machine and CMS detector are very favorable to study this aspect of discovery physics. Furthermore by observing the time development of $B_S^0 - \bar{B}_S^0$ oscillations the mixing parameter χ_S can be measured for values up to 20 [2].

4.6 Quark-gluon plasma search

The heavy ion beams at LHC will provide collision energy densities well above the threshold for the formation of quark gluon plasma (QGP). In this new state of matter all heavy

quark bound states, except for Υ , are suppressed by color screening. The CMS detector has got one of the best muon system. So measurements of $\mu\mu$ pairs rates coming from Υ family can be made to examine the suppression of Υ' and Υ'' relative to Υ in different heavy ion collisions and relative to pp collisions [2]. The CMS detector will be used to detect low momentum muons produced in the heavy ion collisions and reconstruction of Υ , Υ' and Υ'' mesons. In CMS simulation studies the error on the relative suppression factor has been estimated as ≈ 0.2 , ≈ 0.05 and 0.02 for Pb–Pb, Nb–Nb and Ca–Ca collisions respectively.

5. Summary

To summarize the physics potential of LHC is vast. When operational, it would be the only facility in near future to probe and solve present fundamental puzzles of particle physics, namely: Standard Model Higgs boson and/or multiple SUSY Higgs bosons search, SUSY search over entire theoretical allowed mass range, origin of spontaneous symmetry breaking, CP-violation in B -system, substructure of quarks and leptons, etc. The CMS potentials for the search of Standard Model Higgs boson, CP-violation in B -physics and quark gluon plasma searches have been discussed in this talk.

Acknowledgement

The author would like to thank the organizers for inviting him to give this talk. He is also thankful to Dr D Denegri for providing some of the important CMS physics material.

References

- [1] S Dimopoulos and M Lindner, *Proc. of LHC Workshop* Aachen, CERN/90-10 (1990)
C W Fabjan, *LHC: Physics, Machine and Experiments*, CERN-PPE/P95-25 (1995)
- [2] The CMS Collaboration: Technical Proposal, CERN/LHCC 94-38 (1994) and references therein
- [3] The ATLAS Collaboration: *Technical Proposal*, CERN/LHCC 94-39 (1994)
- [4] The ALICE Collaboration: *Letter of Intent*, CERN/LHCC 94-16 (1993)
- [5] The LHCb Collaboration: *Letter of Intent*, CERN/LHCC 95-5 (1995)
- [6] *The CMS Hadron Calorimeter TDR*, CERN/LHCC 97-31 (1997)
- [7] N K Mondal, *The CMS Outer Hadron Calorimeter (HO) EDR*, TIFR/CMS 99-01 (1999)
- [8] S N Ganguli, *Indian J. Phys.* **71**, 41 (1997)
- [9] P Janot, *Indo-French Workshop on SUSY and Unification*, TIFR, Mumbai, 17–21 December, 1997
- [10] H Baer, C Chen, F Paige and X Tata, *Phys. Rev.* **D52**, 2746 (1995)
- [11] W Beenakker, R Hopker, M Spira and P Zerwas, *Nucl. Phys.* **B492**, 51 (1997)
M Spira, hep-ph/9705337
- [12] M Kramer, T Plehn, M Spira and P Zerwas, *Phys. Rev. Lett.* **79**, 341 (1997)
- [13] M Dittmar and H Dreiner, *Phys. Rev.* **D55**, 167 (1997)
- [14] D P Roy, *Pramana – J. Phys.* **51**, 7 (1998)
- [15] I Iashvili, R Kinnunen, A Nikitenko and D Denegri, CMS Note 1995/059, 043 and 101